Self-Organization of TiO_2 Nanoparticles in Thin Films

Shelly D. Burnside,* Valery Shklover, Christophe Barbé, Pascal Comte, Francine Arendse, Keith Brooks, and Michael Grätzel

Laboratory of Photonics and Interfaces, Ecole Polytechnique Fédérale de Lausanne, CH-1015 Lausanne, Switzerland

Received February 24, 1998. Revised Manuscript Received June 9, 1998

Nanocrystalline titanium dioxide colloids have been synthesized using a sol−gel technique followed by growth under hydrothermal conditions in a basic environment at temperatures between 190 and 270 °C. Thin films have been made from aqueous suspensions of these colloids. X-ray analysis showed the colloids to be primarily the anatase crystal phase. Scanning electron microscopy (SEM) revealed a predominantly rodlike particle morphology after growth at lower temperatures and the formation of principally truncated tetragonal or tetrahydral bipyramidal nanocrystallites following growth at higher temperatures. The rodlike particles self-organize into regular cubic arrays with the long axis of the rods aligned perpendicular to the film surface. This self-organization is dependent upon the base used in colloidal synthesis and also upon the dielectric constant of the medium used during film formation.

Introduction

Applications of titanium dioxide colloids and thin films are numerous, including photovoltaic, electrochromic, photochromic, electroluminescence, and catalytic devices and sensors.[1] Recently, sol−gel synthesis of nanocrystalline titanium dioxide and templated amorphous titanium dioxide have been explored by many research groups, including our own.[2−4] We have used both an acidic[5] and a basic environment[6,7] to synthesize sol−gel-derived anatase nanocrystals for use in a dye-sensitized solar cell. Intriguing results have recently been published that show the formation of hexagonally packed, colloidally derived, ordered thin films using a similar sol−gel synthetic scheme in a basic environment.[8] We have independently developed ordered structures of rectangular anatase rods derived from the base-catalyzed sol−gel synthetic scheme, in work described herein. Preliminary results of this work have been previously published.[9]

Ordered structures of materials on the nanometer, micrometer, and millimeter size scale have recently attracted much attention.[10,11] Superlattices of organically passivated nanocrystals have been explored for the possibility of exploiting quantum confinement effects for magnetic and optical applications.[12,13] Additionally, well-ordered superlattices of submicron-sized oxide nanocrystals have been found to yield highly dense ceramic materials following sintering.[14] Order in biomaterials has been intensively studied, with the aim of creating hierarchical structures containing inorganic and organic materials.[15] The importance of order and orientation on properties in synthetic biomaterials has been explored.[16]

Herein, we present work on ordered structures formed from titanium dioxide nanoparticles synthesized using a sol−gel technique. The cause of the ordering phenomena is explored.

Experimental Section

Synthesis. Titanium(IV) isopropoxide (162 mL (0.5 mol), Fluka) was rapidly added to distilled water (290 mL (15.5 mol)) and then stirred for 1 h. A white precipitate formed immediately upon addition of the titanium(IV) isopropoxide. The resultant colloid was filtered using a glass frit and washed

(1) Gerfin, T.; Graetzel, M.; Walder, L. *Molecular and Supramolecular Surface Modification of Nanocrystalline TiO2 Films: Charge-Searating and Charge-Injecting Devices*; Gerfin, T.; Graetzel, M.; Walder, L., Ed.; John Wiley and Sons: 1997; Vol. 44.
(2) Kumar, K.-N. P.; Keizer, K.; Burggraaf, A. J.; Okubo, T.; Nagamoto, H.; Morooka, S. *Nature* **1992**, *358*, 48−50.
(3) O'Regan, B.; Graetzel, M. *Nature* **1991**, *353*, 737−739.
(4) Antonelli, D. M.; Ying, J. Y. *Angew. Chem., Int. Ed. Engl.* **1995**, *34*, 2014−2017.
(5) Barbe, C. J.; Arendse, F.; Comte, P.; Jirousek, M.; Lenzmann, F.; Shklover, V.; Graetzel, M. *J. Am. Cer. Soc.* **1997**, *80*, 3157−3171.
(6) Thomas, I. M. *Appl. Opt.* **1987**, *26*, 4688−4691.
(7) Kay, A.; Graetzel, M. *Solar Energy Mater. Solar Cells* **1996**, *44*, 99−117.
(8) Moritz, T.; Reiss, J.; Diesner, K.; Su, D.; Chemseddine, A. *J. Phys. Chem. B* **1997**, *101*, 8052−8053.
(9) Shklover, V.; Nazeeruddin, M.-K.; Zakeeruddin, S. M.; Barbe, C.; Kay, A.; Haibach, T.; Steurer, W.; Hermann, R.; Nissen, H.-U.; Graetzel, M. *Chem. Mater.* **1997**, *9*, 430−439.
(10) (a) Aksay, I. A.; Trau, M.; Manne, S.; Honma, I.; Yao, N.; Zhou, L.; Fenter, P.; Eisenberger, P. M.; Gruner, S. M. *Science* **1996**, *273*, 892−898. (b) Lu, Y.; Ganguli, R.; Drewien, C. A.; Anderson, M. T.; Brinker, C. J.; Gong, W.; Guo, Y.; Soyez, H.; Dunn, B.; Huang, M. H.; Zink, J. I. *Nature* **1997**, *389*, 364−368. (c) Mann, S.; Ozin, G. A. *Nature* **1996**, *382*, 313−318. (d) Yang, H.; Kuperman, A.; Coombs, N.; Mamiche-Afara, S.; Ozin, G. A. *Nature* **1996**, *379*, 703−705.
(11) (a) Braun, P. B.; Osenar, P.; Stupp, S. I. *Nature* **1996**, *380*, 325−328. (b) Stupp, S. I.; Braun, P. V. *Science* **1997**, *277*, 1242−1248.
(12) Alivisatos, A. P. *Science* **1996**, *271*, 933−937.
(13) Yin, J. S.; Wang, Z. L. *J. Phys. Chem. B* **1997**, *101*, 8979−8983.
(14) Barringer, E. A.; Bowen, H. K. *J. Am. Cer. Soc.* **1982**, *65*, C-199−C-201.
(15) Sarikaya, M.; Aksay, I. A. *Biomimetics: Design and processing of materials*; American Institute of Physics: Woodbury, NY, 1995.
(16) Aksay, I. A.; Baer, E.; Sarikaya, M.; Tirrell, D. A. *Hierarchically Structured Materials*; Materials Research Society: Pittsburgh, 1992; Vol. 255.

S0897-4756(98)00702-9 CCC: $15.00
Published on Web 08/29/1998

three times with 50 mL of distilled water. The filter cake was added to a Teflon-lined titanium autoclave containing 30 mL of either a 0.6 M tetramethylammonium hydroxide (Fluka) or a 0.7 M ammonium hydroxide solution to form a white slurry. The pH of the colloidal solution after addition of base was measured to be between 7 and 8 with pH paper. Peptization in the presence of tetramethylammonium hydroxide occurred after heating the product at 100−135 °C for 3−6 h, whereupon the slurry became a translucent blue-white liquid. Syntheses with ammonium hydroxide did not bring about complete peptization, even after heating at 100−135 °C for periods up to 16 h, and resulted in a milky-white nonviscous solution.

The suspensions which resulted from peptization were treated hydrothermally in the autoclave at temperatures ranging from 190 to 270 °C for 4.5 h. Following growth, the resultant colloidal suspensions were milky white and had a faint fishy odor, indicating some degradation of the tetramethylammonium hydroxide to an amine form. The pH of the resultant colloidal suspension was measured to be between 13 and 13.5. These suspensions were concentrated to form aqeuous solutions containing 45% solids. Films were made from these suspensions by adding one of the following surfactants: TritonX-100 (Aldrich), Brij 35 (BDH Chemicals, Ltd.), hexadecyl trimethylammonium chloride (Kodak), dodecyl sulfate natrium salt (Merck). The resultant solutions contained 0.15−0.5% (wt) surfactant with respect to the titanium dioxide. The films were deposited using a simple doctor-blade technique on a plain glass or conducting glass (Nippon sheet glass coated with fluorine-doped SnO_2) substrate. Additional films were doctor-bladed from colloidal solutions containing no surfactant or containing 0.3 wt % Triton X and 2−23 wt % acetonitrile, with respect to the TiO_2 content. Using a titanium hot plate (Bioblock Scientific), the films were heated under flowing oxygen to 330 °C for 5 min and then to 440 °C for 15 min.

Characterization. The crystallinity and phase of the titanium dioxide was studied with a Siemens powder X-ray diffractometer using Cu Kα radiation. Surface area was determined using a Micromeretics ASAP 2010 nitrogen adsorption−desorption apparatus. Pore size distribution was modeled using the Barrett−Johner−Halenda (BJH) method on the desorption data obtained from the ASAP 2010. Particle morphology and distribution were studied using a Hitachi S-900 field emission microscope, a scanning electron microscope (SEM). Fast Fourier transformations of some images were obtained with software from Digital Micrographs in Pleasonton, CA. High-resolution transmission electron microscopy work (HRTEM) was performed using a Philips CM 30 ST instrument. A thin single-crystal gold film was used as the internal standard for the determinaton of interplanar distances. Samples of a sintered colloid which had been powdered were dispersed in a heptane solution, into which a copper TEM grid was dipped.

Results and Discussion

Three phases of titanium dioxide (TiO_2) have been commonly observed: anatase, brookite, and rutile.[17] X-ray diffraction patterns from samples synthesized herein (Figure 1) show the formation of anatase particles after peptization and after further autoclaving at temperatures between 190 and 270 °C. In the samples measured following peptization and after autoclaving at temperatures below 210 °C, a broad peak is observed in the vicinity of the most intense peak for the brookite crystal phase, perhaps indicating the presence of small amounts of brookite. This peak is not present in samples autoclaved at higher temperatures. The formation of rutile is not observed, as noted by the flat background in the region of the two most intense rutile peaks. This has also been confirmed by TEM analysis, as discussed later. Anatase is the preferred crystal form of titanium dioxide for many applications, including lithium insertion batteries, electrochromic devices, and dye-sensitized solar cells.[1] The X-ray diffraction peaks broaden with decreasing autoclaving temperature, indicating decreasing particle size, with the broadest peaks observed for the sample measured following peptization. This trend is confirmed by nitrogen adsorption−desorption data, as modeled using the BET equation to give surface area. (Table 1) Over the temperature range investigated, the surface area following autoclaving decreases from 66 to 35 m^2/g, indicating the growth of larger particles from the smallest, highest surface area (188 m^2/g) nanocrystallites which are formed after peptization. The titanium dioxide synthesized herein differs from titanium dioxide nanocrystallites synthesized in an acidic environment (pH = 1), which exhibit traces of rutile formation at autoclaving temperatures above 250 °C and larger surface areas.[5] The effect of catalyst pH on the formation of titanium dioxide is similar to that observed for sol−gel-derived silica, where base-catalyzed colloids

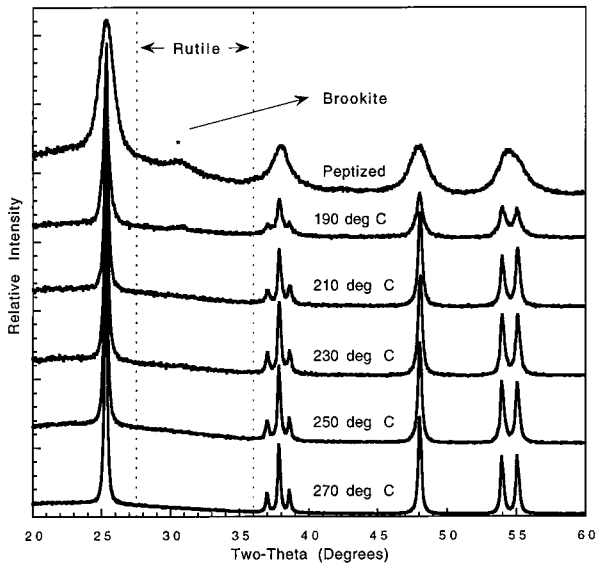

Figure 1. X-ray diffraction patterns for nanocrystalline titanium dioxide colloids after pepization and after autoclaving between 190 and 270 °C. The position of the two most intense peaks for rutile and the most intense peak for brookite are noted. All peaks in the XRD pattern can be identified as the anatase crystal phase of titanium dioxide, except for the weak peak near the most intense peak for brookite.

Table 1. Surface Area Analysis, Pore Size Analysis, and Porosity of Films Derived from Nanocrystalline Titanium Dioxide Colloids Autoclaved at Various Temperatures

autoclaving temp (°C)	surface area (m^2/g)	average pore diameter (nm)	porosity (%)
following peptization	188.5		
190	66.1	3.5[a]	26[a]
210	61.2	3.8[a]	27[a]
230	50.3	8.5[a]	29[a]
250	38.9	30[b]	42[b]
270	35.0	35[b]	44[b]

[a] Prepared at a concentration of 2.9×10^{-3} g of Triton X-100/g of TiO_2 from a solution containing 42 wt % TiO_2 [b] Prepared at a concentration of 2.9×10^{-3} g of Triton X-100/g of TiO_2 from a solution containing 50 wt % TiO_2

(17) Barksdale, J. *Titanium: Its Occurrence, Chemistry, and Technology*; Ronald Press: New York, 1949.

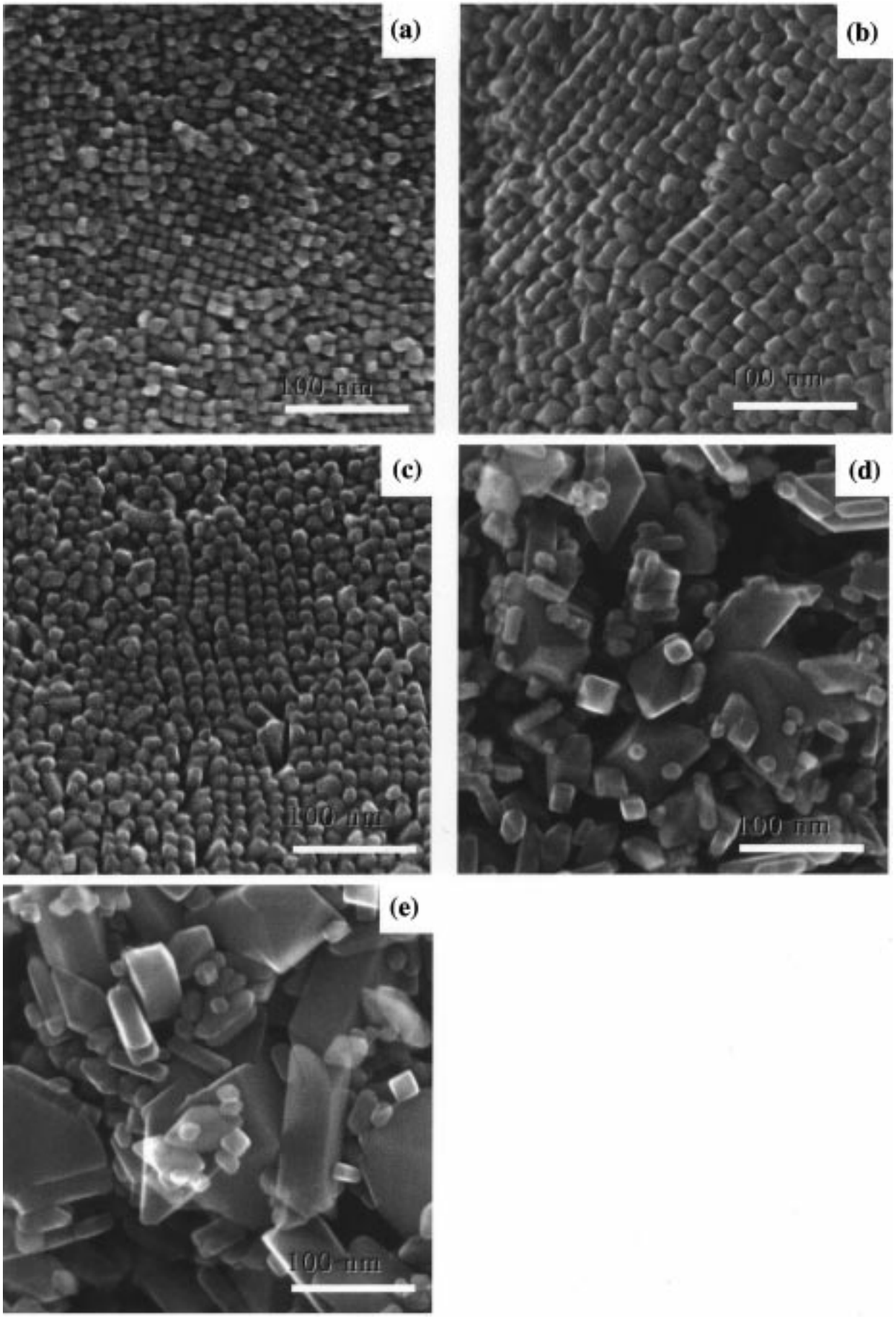

Figure 2. SEM micrographs of thin films deposited using a colloid autoclaved at (a) 190, (b) 210, (c) 230, (d) 250, and (e) 270 °C containing 0.15 wt % Triton X-100 with respect to the titanium dioxide.

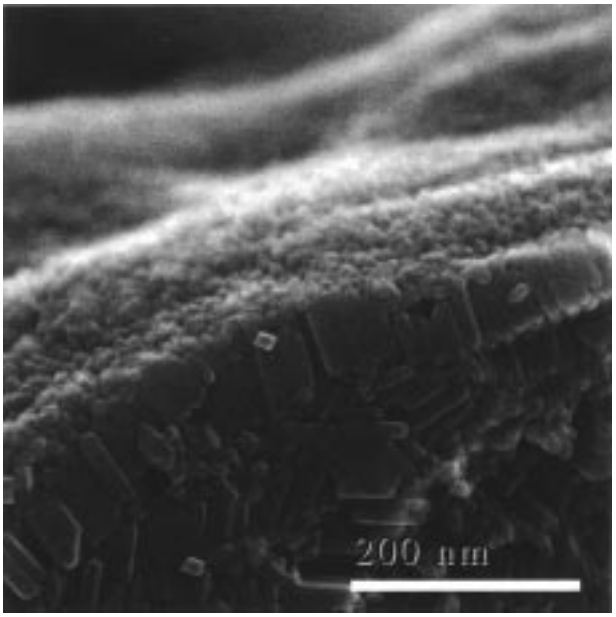

Figure 3. SEM cross-sectional micrograph of thin film deposited using a colloid autoclaved at 210 °C, containing 0.15 wt % Triton X-100 with respect to the titanium dioxide.

exhibit lower surface areas than those catalyzed with acid.[18]

SEM analysis also shows the increase in particle size as a function of temperature, indicated in Figure 2. Moreover, the predominant crystal habit changes from a rodlike prismatic species (hereafter referred to as rods) to a tetrahydral bipyramidal or truncated tetragonal species. At higher temperatures, these morphologies coexist, with a preponderance of bipyramids. Growth of colloids occurs by two mechanisms: dissolution of smaller, more soluble particles, accompanied by reprecipitation on and growth of larger particles (Ostwald ripening), or agglomeration of smaller, primary particles to form larger particles.[18,19] We suggest that the latter mechanism causes growth in this case, as agglomerates of the primary, rod-shaped particles can be observed in Figure 2e. Moreover, it has been suggested in earlier studies of sol−gel-derived TiO_2 that primary particle agglomeration is the primary growth mechanism.[20]

The SEM micrographs in Figure 2a−c also exhibit regions containing regularly ordered structures of the rodlike particles synthesized at lower temperatures (190−230 °C). Each rod is in contact with four additional rods in the equatorial plane, as described previously.[9] Cross sectional SEM analysis of these ordered materials show two to three layers of these aligned rods, with occasional interleavings of the larger bipyramids. (Figure 3) The samples autoclaved at higher temperatures contain a higher number of the larger bipyramids, which frustrates the regular ordering of the rods, creating more random structures.

High-resolution transmission electron microscopy (HR-TEM) was performed to elucidate the surface planes of the titanium dioxide particles. (Figure 4). The rodlike particles, which order regularly and are indicated in region A, were observed to have (100) faces, irregularly terminated from (001) side. The tetragonal and bipyramidal particles have primarily (101) surfaces, as observed previously for anatase nanocrystallites.[9] These (001) and (101) faces are the typically observed surface for naturally occurring anatase.[21] We suggest that these particles may have properties useful for studying the effect of surface on adsorption of dye for the dye-sensitized solar cell or for adsorption of other organic molecules as used in catalytic systems.

The ordered structures formed in films from particles autoclaved at 230 °C or below create extremely narrow pore size distributions, as observed in Figure 5 and Table 1. For the sample autoclaved at 190 °C, the pore size distribution even approaches monodispersity. The packing of the rodlike nanocrystallites creates extremely regular, narrow channels that may serve as electronic junctions or for use in membranes.[22,23] The close packing of the particles is also reflected in the extremely low porosities observed for samples autoclaved at 230 °C or below (Table 1). These samples show a pore size distribution and porosity which is very similar to the distribution in sol−gel derived silica xerogels and mesoporous molecular sieves.[4,18] The nonordered structures formed by the particles autoclaved at 250 and 270 °C do not exhibit narrow pore size distributions or low porosities, due to their inability to form a close-packed structure. The concentration of the solution used to form the films from these larger particles was lower due to the high viscosity of the colloidal solutions which prevented good mixing of the surfactant solution when not diluted. When the ordered samples were diluted to similar concentrations and analyzed, the porosity values remained the same, though the pore size distribution widened.

Other researchers have also observed ordering of submicron-sized particles, including nanocrystalline titanium dioxide, arising from a variety of causes. Hexagonal-shaped sol−gel-derived anatase crystals were observed to pack in a hexagonal close-packing arrangement.[8] These particles were synthesized using a similar synthetic scheme as described herein, but without the hydrothermal growth step and at a lower pH, resulting in smaller (13 nm) hexagonal slabs. The ordering of the hexagonal nanocrystals was suggested to result from the directing forces of the organic base used as a catalyst. Self-assembly and organization were also observed to occur when hydrogen-bonding and -accepting ligands were attached to spherical titanium dioxide nanocrystallites.[24,25] Sol−gel-derived anatase or amorphous precursors of densely packed rutile thin films have also been reported to form uniformly close-packed structures,

(18) Brinker, C. J.; Scherer, G. W. *Sol−Gel Science*; Academic Press: Boston, 1990.
(19) Nielsen, A. E. *Kinetics of Precipitation*; Pergamon Press: Oxford, 1964.
(20) Dirksen, J. A.; Ring, T. A. *Production of Powders for High-Tech Ceramics*; Dirksen, J. A.; Ring, T. A., Ed.; Academic Press: New York, 1989; pp 29−39.
(21) Ramdohr, R.; Strunz, H. *Klockmans Lehrbuch der Mineralogie*; Enke Verlag: Stuttgart, 1978.
(22) Gratzel, M. Nanocrystalline Electronic Junctions. In *Semiconductor Nanoclusters: Physical, Chemical, and Catalytic Aspects*; Kamat, P. V., Meisel, D., Eds.; Elsevier: Amsterdam, 1996; Vol. 103; pp 353−375.
(23) Guizard, C.; Julbe, A.; Larbot, A.; Cot, L. Ceramic Membrane Processing. In *Chemical Processing of Ceramics*; Lee, B. I., Pope, E. J. A., Eds.; Marcel Dekker: New York, 1994; pp 501−531.
(24) Cusack, L.; Rizza, R.; Gorelov, A.; Fitzmaurice, D. *Angew. Chem., Int. Ed. Engl.* **1997**, *36*, 848−851.
(25) Rizza, R.; Fitzmaurice, D.; Hearne, S.; Hughes, G.; Spoto, G.; Ciliberto, E.; Kerp, H.; Schropp, R. *Chem. Mater.* **1997**, *9*, 2969−2982.

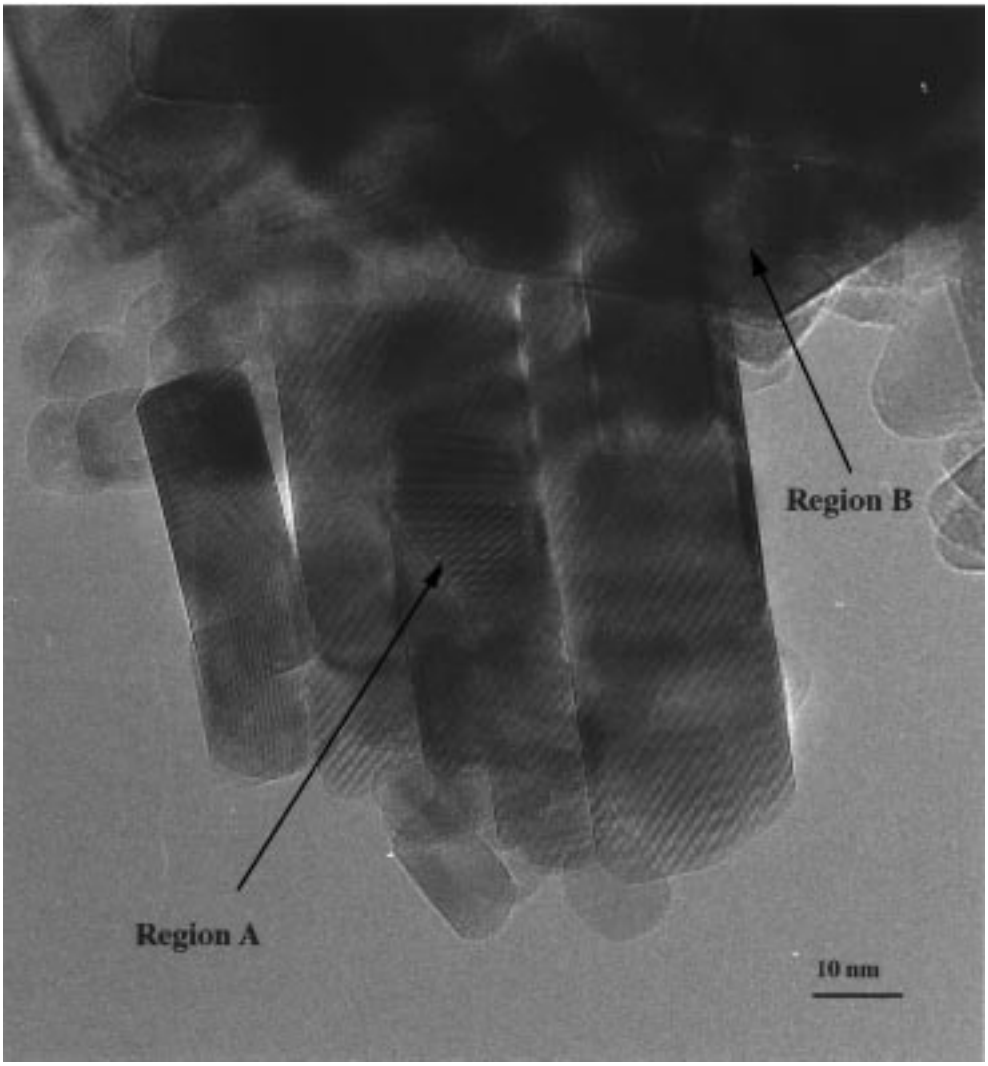

Figure 4. HRTEM micrograph of rodlike anatase particles (region A) which exhibit (100) faces and a tetragonal particle which exhibits (101) faces (region B).

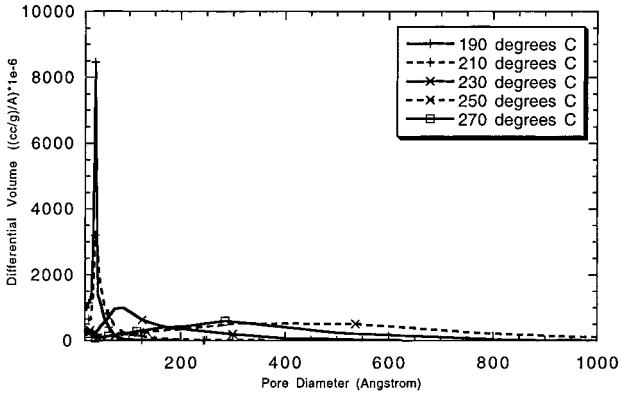

Figure 5. Pore size distribution as determined using desorption data and the BJH model for films deposited using a colloid autoclaved at 190, 210, 230, 250, and 270 °C containing 0.15 wt % Triton X-100 with respect to the titanium dioxide.

due to capillary forces.[26,27] Poly(vinyl chloride) swollen with titanium alkoxides formed aligned rods of rutile upon pyrolysis of the polymer at elevated temperatures, with the alignment resulting from elongation of the polymer in the swollen state.[28] Spherical zinc oxide has been observed to form close-packed structures.[9] Electrophoretic deposition of colloidal latex particles or silicon spheres resulted in hexagonally close-packed structures.[29]

We suggest that, in this work, the ordering phenomena is caused by balanced attractive and repulsive forces, as described by the classic Derjaguin−Landau−Verwey−Overbeek (DLVO) Theory. The DLVO theory has been invoked earlier to explain ordering observed in films and concentrated suspensions of latex and gold particles.[26] We propose that the balancing of these forces arises from the stabilizing and directing ability of the tetramethylammonium hydroxide, as proposed in earlier work.[8] The system used herein was not model enough to allow quantitative application of DLVO theory, so only qualitative analyses were performed. Titanium dioxide was synthesized in the presence of ammonium hydroxide, a base with a lower effective

(26) Kumar, K.-N. P.; Keizer, K.; Burggraaf, A. J.; Okubo, T.; Nagamoto, H.; Morooka, S. *Nature* **1992**, *358*, 48−50.
(27) Barringer, E. A.; Bowen, H. K. *J. Am. Cer. Soc.* **1982**, *65*, C-199−C-201.
(28) Burdon, J.; Calvert, P. *Orientation in Biomimetic Polymer-Mineral Composites*; Burdon, J.; Calvert, P., Ed.; Materials Research Society: Pittsburgh, 1992; Vol. 255, pp 375−383.
(29) (a) Giersig, M.; Mulvaney, P. *Langmuir* **1993**, *9*, 3408−3413. (b) Giersig, M.; Ung, T.; Liz-Marzan, L. M.; Mulvaney, P. *Adv. Mater.* **1997**, *9*, 570−575.

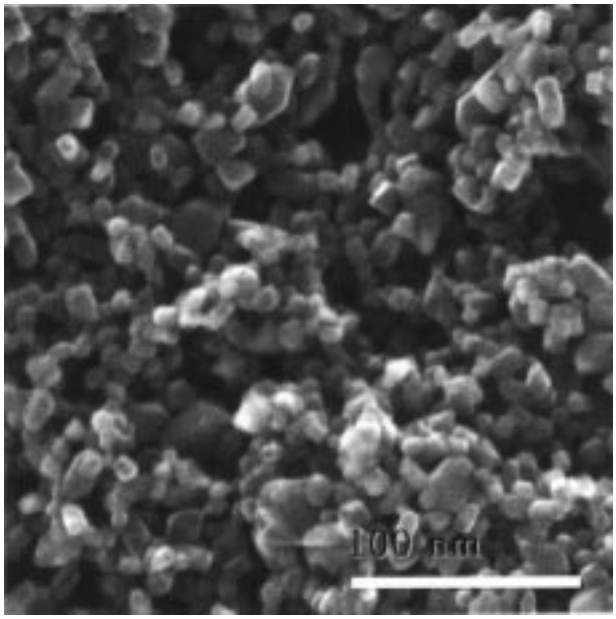

Figure 6. SEM micrographs of thin film of titanium dioxide colloid synthesized in the presence of ammonium hydroxide and autoclaved at 210 °C for 4.5 h.

electrostatic radius and lower polarizability. The effective electrostatic radii of tetramethylammonium hydroxide and ammonium hydroxide have been estimated to be 0.51625 and 0.151 nm, respectively.[30] The Stern layer, the compact layer of ions immobilized on the colloidal surface, will be larger and more polarizable for the tetramethylammonium hydroxide containing colloid than for the ammonium hydroxide containing colloid.[31] The resulting SEM micrographs revealed no ordering (Figure 6). We suggest that the ammonium hydroxide leads to an increased rate of flocculation and agglomeration of the colloidal particles during film formation, leading to disordered films.

Additionally, another set of experiments was performed in which acetonitrile was added to the colloidal suspension containing Triton X. The addition of acetonitrile lowers the dielectric constant of the solvent, the propagating medium for attractive and repulsive forces between the colloidal particles. The acetonitrile-containing suspensions were analyzed at acetonitrile concentrations ranging from 2 to 23 wt % with respect to the titanium dioxide content. Micrographs of films from suspensions containing less than 23% acetonitrile showed some regions of ordered particles, but at larger concentations, the films contained fewer ordered regions (Figure 7). Fast Fourier transforms (FFT) of representative areas of these ordered and nonordered images have been performed (Insets of Figure 7). The ordered samples display a crosslike figure following Fourier transformation, reflecting the regular packing of the particles. The nonordered samples show no signs of correlation between the particles, resulting in a featureless Fourier transform. The influence of acetonitrile on ordering suggests a disruption of the balanced attractive and repulsive forces between the colloidal particles, causing flocculation and agglomeration during film formation.

To form films which adhered well to the substrate, it was found necessary to add a surfactant to the colloidal suspension before doctor-blading. To probe the effect of surfactant upon the ordering phenomena, experiments were performed with four types of surfactants: an anionic surfactant (dodecylsodium sulfate), a cationic surfactant (hexadecyltrimethylammonium chloride), and two nonionic surfactants (Triton X-100 and Brij 35) over a concentration range varying from 0.05 to 0.2 wt % surfactant with respect to the TiO_2. These experiments showed the formation of ordered regions at all concentrations and types of surfactants. The surfactant loading used at all levels is much less than a monolayer. To further probe the role of the surfactant, a sample was imaged containing no surfactant. The film adhered poorly to the substrate, but in the regions which could be imaged, SEM micrographs revealed order. We conclude that the surfactant has very little effect upon the ordering phenomena observed herein.

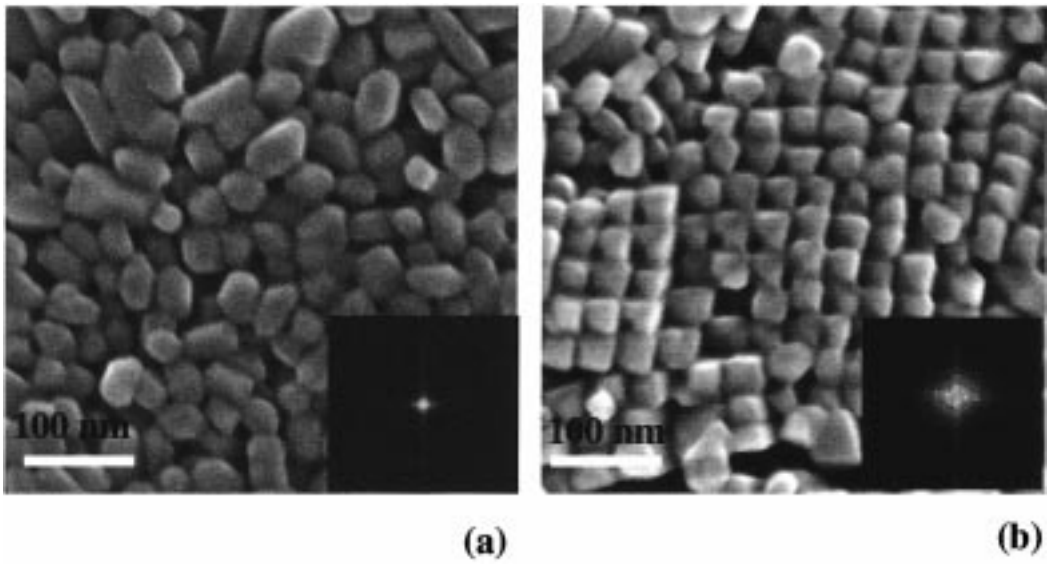

Figure 7. Representative areas of SEM images from TiO_2 films desposited from colloidal suspensions containing (a) 0 and (b) 23 wt % acetonitrile with respect to the titanium dioxide content in addition to 2.9×10^{-3} g of Triton X-100/g of TiO_2. The insets show Fast Fourier Transforms of the SEM images.

Conclusion

Ordered titanium dioxide thin films have been prepared from colloids autoclaved at temperatures between 190 and 230 °C. X-ray diffraction shows these films to be titanium dioxide of only the anatase phase. Nitrogen adsorption−desorption measurements show that the structures exhibit extremely low porosities, with narrow pore size distributions.

We suggest that the ordering in these films is caused by balanced attractive and repulsive interactions of the tetramethylammonium-coated surfaces in an aqueous medium. This suggestion has been tested by varying the base, to vary the surface coating, and also by varying the dielectric constant of the colloidal medium, and both have shown to result in nonordered structures. The presence of surfactant, necessary to produce crack-free films, has not been observed to play a role in the ordering phenomenon.

We are currently exploring the feasibility and merits of these structures for use in lithium insertion batteries[32] and for the dye-senstized solar cell 5.[33] We also suggest that these ordered structures may serve well as catalysts, as recent work has shown that bundles of anatase tubules are more effective catalysts than thin film anatase for the photodecomposition of salicyclic acid.[34] The preponderance of (100) surface planes observed in these samples may also have beneficial effects upon the performance of these colloids as compared to traditional anatase.

Acknowledgment. The authors thank Dr. P. Infelta for many helpful and stimulating conversations and R. Wessicken for recording the HRTEM patterns. The SEM measurements were performed at the Laboratory of Electron Microscopy (ETH—Zürich) and the HRTEM measurements at the Laboratory of Solid State Physics (ETH—Hönggerberg). Funding for this project was provided by a European Union Joule Project (JOR3-CT97-0147: Dye Photovoltaic Cells for Indoor Applications).

CM980702B

(30) Sahai, N.; Sverjensky, D. A. *Geochim. Cosmochim. Acta* Submitted.
(31) Ross, S.; Morrison, I. D. *Colloidal Systems and Interfaces*; John Wiley and Sons: New York, 1988.
(32) (a) Kavan, L.; Graetzel, M.; Rathousky, J.; Zukal, A. *J. Elec. Soc.* **1996**, *143*, 394−400. (b) Kavan, L.; Graetzel, M.; Gilbert, S. E.; Klemenz, C.; Scheel, H. J. *J. Am. Chem. Soc.* **1996**, *118*, 6716−6723.
(33) O'Regan, B.; Graetzel, M. *Nature* **1991**, *353*, 737−739.
(34) Lakshmi, B. B.; Dorhout, P. K.; Martin, C. R. *Chem. Mater.* **1997**, *9*, 857−862.